

## Important Notice to Authors

Attached is a PDF proof of your forthcoming article in Optics Express. The article Manuscript ID is 455542. *No further processing of your paper will occur until we receive your response to this proof.*

**Note:** *Excessive proof corrections submitted by the author can result in significant delays to publication. Please include only essential changes that might be needed to address any shortcomings noticed in the proof-preparation process.*

### Author Queries

Please answer these queries by marking the required corrections at the appropriate point in the text or referring to the relevant line number in your PDF proof.

Q1	The funding information for this article has been generated using the information you provided to us at the time of article submission. Please check it carefully. If any information needs to be corrected or added, please provide the full name of the funding organization/institution as provided in the Crossref Open Funder Registry ( <a href="https://search.crossref.org/funding">https://search.crossref.org/funding</a> ).
----	--

### Other Items to Check

- Please note that the original manuscript has been converted to XML prior to the creation of the PDF proof, as described above. The PDF proof was generated using LaTeX for typesetting. The placement of your figures and tables may not be identical to your original paper.
- Please carefully check all key elements of the paper, particularly the equations and tabular data.
- Author list: Please make sure all authors are presented, in the appropriate order, and that all names are spelled correctly.
- If you need to supply new or replacement figures, please upload each figure as an individual PDF file at the desired final figure size. The figure must fit inside the margins of the manuscript, i.e., width no more than 5.3 inches (or 13.46 cm). Confirm the quality of the figures and upload the revised files when submitting proof corrections.

# Absolute clock synchronization with a single time-correlated photon pair source over a 10 km optical fibre

JIANWEI LEE,<sup>1</sup> LIJIONG SHEN,<sup>1</sup>  ADRIAN NUGRAHA UTAMA,<sup>1</sup> AND CHRISTIAN KURTSIEFER<sup>1,2,\*</sup> 

<sup>1</sup>Centre for Quantum Technologies, National University of Singapore, 3 Science Drive 2, Singapore 117543, Singapore

<sup>2</sup>Department of Physics, National University of Singapore, 2 Science Drive 3, Singapore 117551, Singapore

\*christian.kurtsiefer@gmail.com

**Abstract:** We demonstrate a point-to-point clock synchronization protocol based on bidirectionally propagating photons generated in a single spontaneous parametric down-conversion (SPDC) source. Tight timing correlations between photon pairs are used to determine the single and round-trip times measured by two separate clocks, providing sufficient information for distance-independent absolute synchronization secure against symmetric delay attacks. We show that the coincidence signature useful for determining the round-trip time of a synchronization channel, established using a 10 km telecommunications fiber, can be derived from photons reflected off the end face of the fiber without additional optics. Our technique allows the synchronization of multiple clocks with a single reference clock co-located with the source, without requiring additional pair sources, in a client-server configuration suitable for synchronizing a network of clocks.

© 2022 Optica Publishing Group under the terms of the [Optica Open Access Publishing Agreement](#)

## 1. Introduction

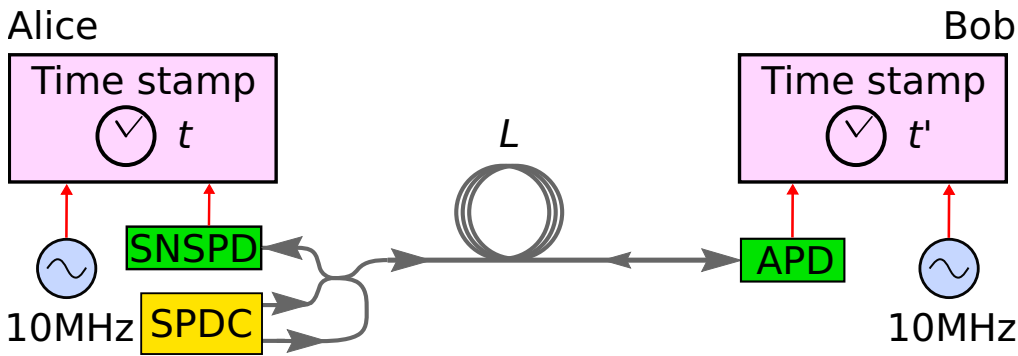
Complementary to clock recovery schemes from data streams, absolute clock synchronization protocols, e.g. network time protocol (NTP), precision time protocol (PTP), two-way satellite time transfer (TWSTT), are widely-used to determine the offset between physically separated clocks [1–4]. By exchanging counter-propagating signals, and assuming a symmetric synchronization channel, parties estimate one-way propagation delays as half the round-trip time signals without characterizing their physical separation beforehand. Spatially separated parties then deduce their absolute clock offset by comparing signal propagation times measured with their devices with the expected propagation delay [5]. Recently, protocol implementations with entangled photon pairs suggest securing the synchronization channel by measuring non-local correlations – a technique inspired by entanglement-based quantum key distribution (QKD) [6–8]. With independent hydrogen-maser and rubidium clocks as references, the protocol has a demonstrated timing stability limited to the intrinsic instability of the clocks over 7 km [9], and is secure against symmetric-delay attacks [6]. However, to realize a bidirectional exchange of photons, these demonstrations required a photon pair source at each end of the synchronization channel, posing a resource challenge when synchronizing multiple clocks.

In this work, we experimentally demonstrate a bidirectional clock synchronization protocol where the synchronization channel is established with a 10 km optical fiber and a single entangled photon pair source. The round-trip time is sampled using time-correlation measurements between the detection times of photon pairs, with one photon of the pair back-reflected at the remote side using the end face of the fiber. We demonstrate a distance-independent synchronization of two separated clocks, referenced to independent rubidium frequency standards. Already from a quite modest photon pair detection rate of  $160\text{ s}^{-1}$  we obtain a precision sufficient to resolve clock

52 offset fluctuations with an uncertainty of 88 ps in 100 s, consistent with the intrinsic frequency  
 53 instability between our clocks.  
 54

## 55 2. Time synchronization protocol

56 The protocol involves two parties, Alice and Bob, connected by a single mode optical fiber (see  
 57 Fig. 1). Alice has an SPDC source producing photon pairs, one photon is detected locally, while  
 58 the other is sent and detected on the remote side. Occasionally, the transmitted photon undergoes  
 59 Fresnel reflection ( $R \approx 3.5\%$ ) at the end face of the fiber, and is eventually detected by Alice  
 60 instead. Every photodetection event is time tagged according to a local clock which assigns time  
 61 stamps  $t$  and  $t'$  at Alice and Bob, respectively.  
 62



75 **Fig. 1.** Clock synchronization setup. Alice has a source of time-correlated photon pairs  
 76 based on spontaneous parametric down-conversion (SPDC) and a single-photon nanowire  
 77 photodetector (SNSPD). One photon of the pair is detected locally, while the other one is  
 78 sent through a single mode fiber of length  $L$  to be detected on the remote side with Bob's  
 79 InGaAs avalanche photodiode (APD). Times of arrival for all detected photons are recorded  
 80 at each side with respect to the local clock, each locked to a rubidium frequency reference  
 81 (10 MHz). Occasionally, a transmitted photon is reflected at the end face of the fiber back to  
 82 Alice, allowing her to determine the round-trip time and derive the absolute offset between  
 83 the clocks.

84 Photon pairs emerging from SPDC are tightly time-correlated ( $\approx 100$  fs) [10]. Thus, for an  
 85 offset  $\delta$  between the clocks, a propagation time  $\Delta t_{AB}$  from Alice to Bob, and  $\Delta t_{BA}$  in the other  
 86 direction, the second-order correlation function [11]  $G^{(2)}(\tau)$  of the time difference  $\tau = t' - t$  has  
 87 a peak at

$$88 \quad \tau_{AB} = \delta + \Delta t_{AB} \quad (1)$$

89 due to pairs detected at opposite ends of the channel, whereas for two photons detected by Alice  
 90 at  $t$  and  $t + \tau$ , the auto-correlation function  $R(\tau)$  will show a peak at

$$92 \quad \tau_{AA} = \Delta t_{AB} + \Delta t_{BA}, \quad (2)$$

94 corresponding to the round-trip time of the channel. If the propagation times in the two directions  
 95 are the same,  $\Delta t_{AB} = \Delta t_{BA}$ , the the clock offset can be deduced directly from the positions of the  
 96 two peaks using

$$98 \quad \delta = \tau_{AB} - \frac{1}{2} \tau_{AA}, \quad (3)$$

99 independently of the propagation time  $\Delta t_{AB}$ . In this way, the protocol is inherently robust against  
 100 symmetric changes in channel propagation times.  
 101

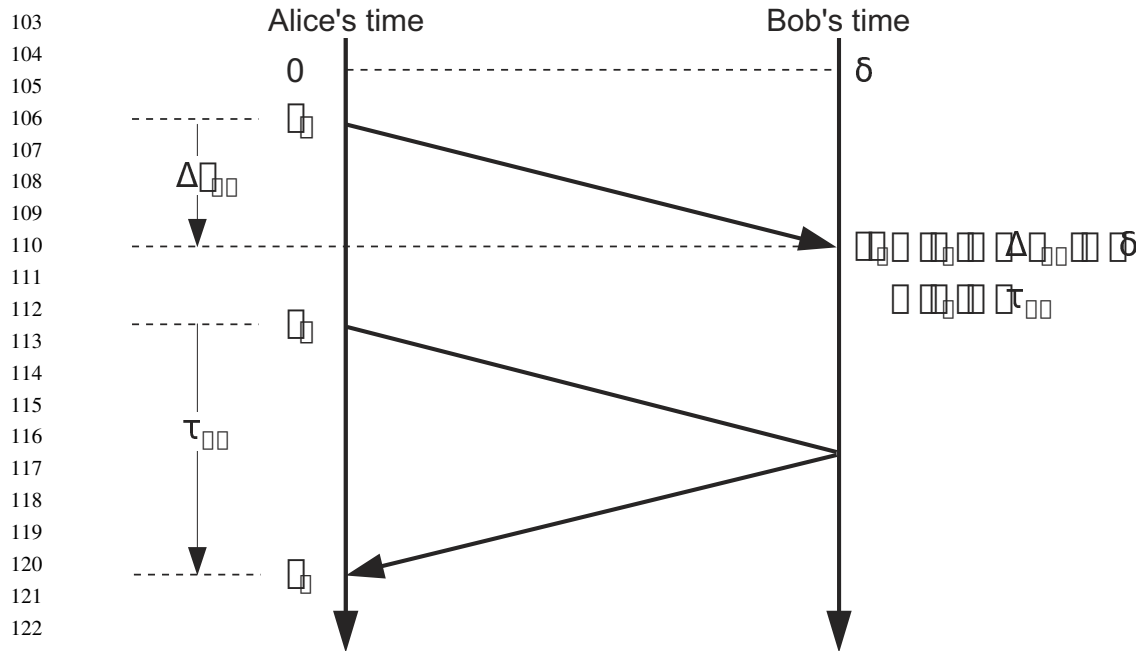


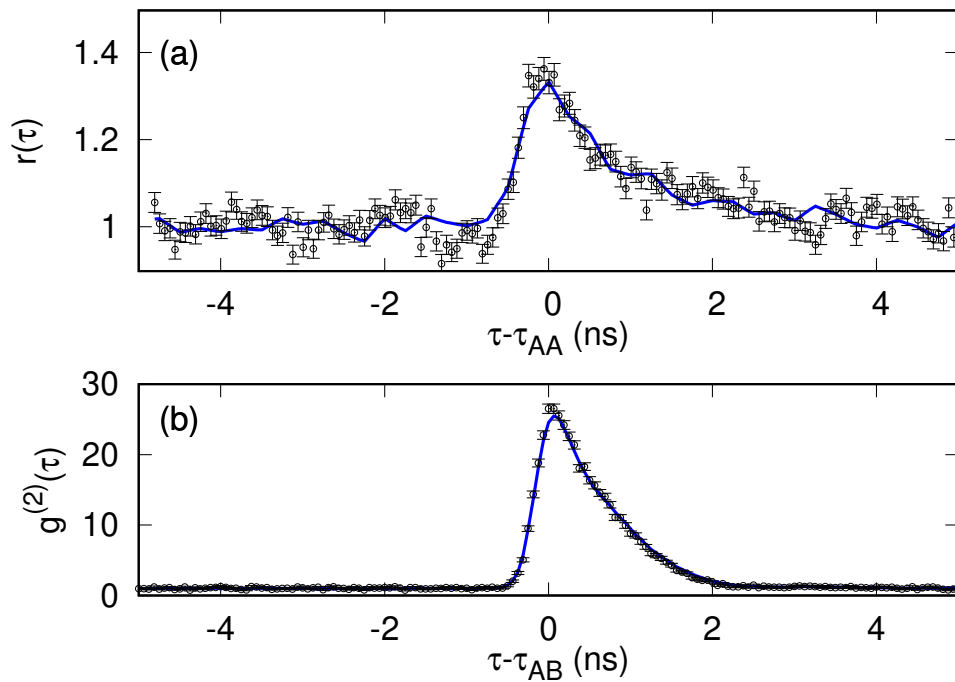
**Fig. 2.** Clock synchronization scheme. Alice and Bob measure detection times  $t$  and  $t'$  of photon pairs generated from Alice's source using local clocks. Detection times  $t_1$  and  $t'_2$  are associated with a time-correlated photon pair where one photon of the pair is transmitted to Bob, while  $t_3$  and  $t_4$  are associated with a pair where one of the photons is reflected at Bob back to Alice. The single-trip time  $\tau_{AB}$  of photons in the synchronization channel, calculated from the time difference  $t'_2 - t_1$ , depends on the signal delay  $\Delta t_{AB}$  associated with the length of the channel, and the absolute clock offset  $\delta$  between the clocks. The round-trip time  $\tau_{AA}$  of the channel is estimated using  $t_4 - t_3$ . Assuming a symmetric delay channel,  $\delta$  can be derived from  $\tau_{AB}$  and  $\tau_{AA}$  without *a priori* knowing  $\Delta t_{AB}$ .

### 3. Experiment

A sketch of the experimental setup is shown in Fig. 1. Our photon pair source [12–14] is based on Type-0 SPDC in a periodically-poled crystal of potassium titanyl phosphate (PPKTP) pumped by a laser diode at 658 nm (Ondax, stabilized with holographic grating). The resulting photon pairs are degenerate at 1316 nm, close to the zero dispersion wavelength of the synchronization channel (SMF-28e, 10 km), with a bandwidth of  $\approx 50$  nm on either side of this wavelength [14]. Signal and idler photons are efficiently separated using a wavelength division demultiplexer (WDM). Fiber beam splitters separate the photon pairs so that one photon is detected locally with a superconducting nanowire single-photon detector (SNSPD, optimized for 1550 nm), while the other photon is routed into the synchronization channel where it is detected on the remote side with an InGaAs avalanche photodiode (APD). The SNSPD has relatively low jitter ( $\approx 40$  ps) compared to APDs ( $\approx 300$  ps), and allows Alice to measure the round-trip time more accurately regardless of the choice of detector by the remote party. With a pump power of 2.5 mW focused to a beam waist of  $140\ \mu\text{m}$  at the centre of the crystal, we observed pair rates of  $160\ \text{s}^{-1}$  and  $8900\ \text{s}^{-1}$  associated with the round-trip and single-trip propagation of photons, respectively.

Photon detection times  $t$  and  $t'$  at Alice and Bob are registered with a nominal resolution of  $\approx 4$  ps. We compute [15] the histograms  $G^{(2)}(\tau)$  and  $R(\tau)$  with a bin width of  $62.5$  ps, and observed coincidence peaks associated with the single-trip and round-trip propagating photons (FWHM = 905 ps and 950 ps, respectively). Figure 3 shows the respective histograms normalized

154 to background coincidences when the two clocks are locked to a common rubidium frequency  
 155 reference (Stanford Research Systems FS725), separated by a fiber spool of constant length  
 156  $L = 10$  km. To deduce the clock offset, we first generate empirical models (Fig. 3, solid-lines) for  
 157 the two coincidence peaks using 100 s of timestamp data – the models are used to fit subsequent  
 158 histograms to extract peak positions  $\tau_{AB}$  and  $\tau_{AA}$ . With the peak positions, we then determine the  
 159 clock offset using Eqs. (2) and (3). To characterize the synchronization precision  $\delta t$  as a function  
 160 of the acquisition time, we measure the standard deviation of twenty offset measurements, each  
 161 extracted from time stamps recorded for a duration  $T_a$ . Figure 4 shows the precision of the  
 162 measured offset, single-trip ( $\tau_{AB}$ ) and round-trip times ( $\tau_{AA}$ ). We observe that the precision for the  
 163 single and round-trip times improves with  $T_a$  for timescales  $\lesssim 100$  s, but deteriorates for longer  
 164 timescales. We attribute this effect to temperature-dependent ( $\Delta T = 45$  mK over 1 min, 160 mK  
 165 over 3 hours) length fluctuations, given that the propagation delay variation [16] of our fiber is  
 166 several  $10 \text{ ps km}^{-1} \text{ K}^{-1}$ . However, we observe that these long-term fluctuations are suppressed in  
 167 the clock offset measurement with the distance-independent synchronization protocol.  
 168



189 **Fig. 3.** Timing correlations showing coincidence peaks due to (a) round-trip and (b) single-  
 190 trip propagation of photons in the synchronization channel. (a)  $r(\tau)$ : auto-correlation function  
 191  $R(\tau)$  normalized to background coincidences extracted from Alice's timestamps acquired  
 192 over 100 s. (b)  $g^{(2)}(\tau)$ : cross-correlation function  $G^{(2)}(\tau)$  normalized to background  
 193 coincidences extracted from Alice and Bob's timestamps acquired over 3 s. Solid lines: fits  
 194 to heuristic model.  $\tau_{AA}$  and  $\tau_{AB}$ : peak positions of respective distributions. Error bars:  
 195 propagated Poissonian counting statistics.  
 196

197 For subsequent demonstrations, we set  $T_a = 3$  s and 90 s for the single and round-trip time  
 198 measurements, obtaining a precision of 12 ps and 14 ps, respectively. Each 90 s window used  
 199 to evaluate the round-trip time thus contains thirty single-trip time measurements. For each  
 200 single-trip time value, we evaluate the clock offset using the round-trip time evaluated in the  
 201 same window. This results in a precision of 16 ps for the measured offset. Measuring the  
 202 single-trip delay with shorter  $T_a$  enables frequent measuring of  $G^{(2)}(\tau)$ , and is useful for tracking  
 203

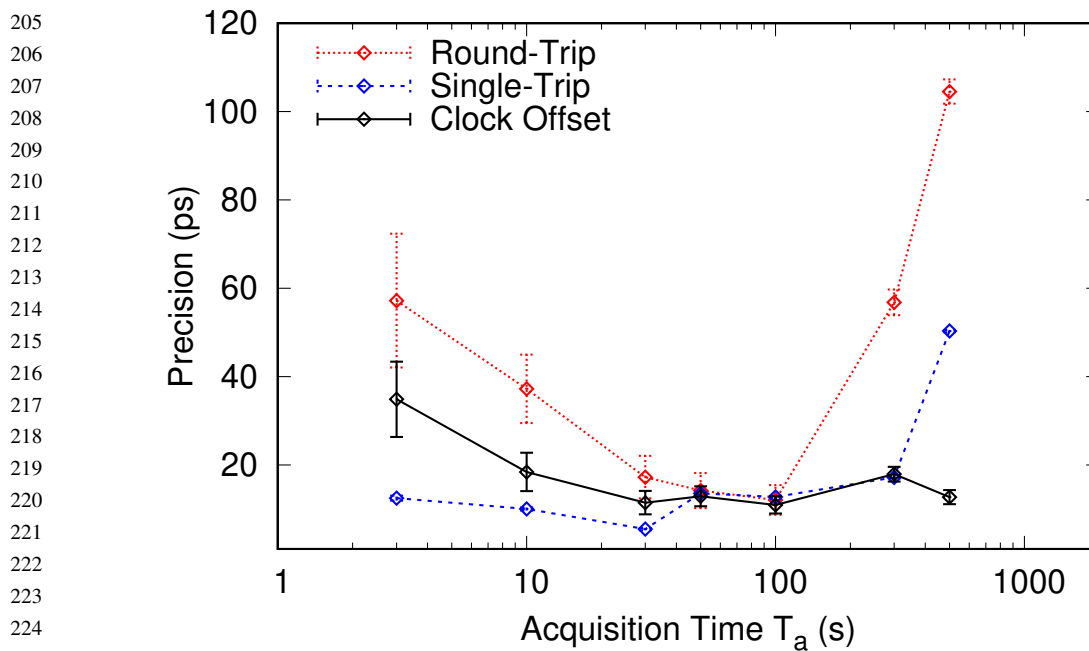


**Fig. 4.** Precision of the round-trip (red) and single-trip (blue) times, and the clock offset (black) between two clocks. Both clocks are locked to the same frequency reference. Error bars: precision uncertainty due to errors in determining the positions,  $\tau_{AB}$  and  $\tau_{AA}$ , of the coincidence peaks.

the position of its coincidence peak ( $\tau_{AB}$ ) in the scenario where clocks are locked to independent frequency references.

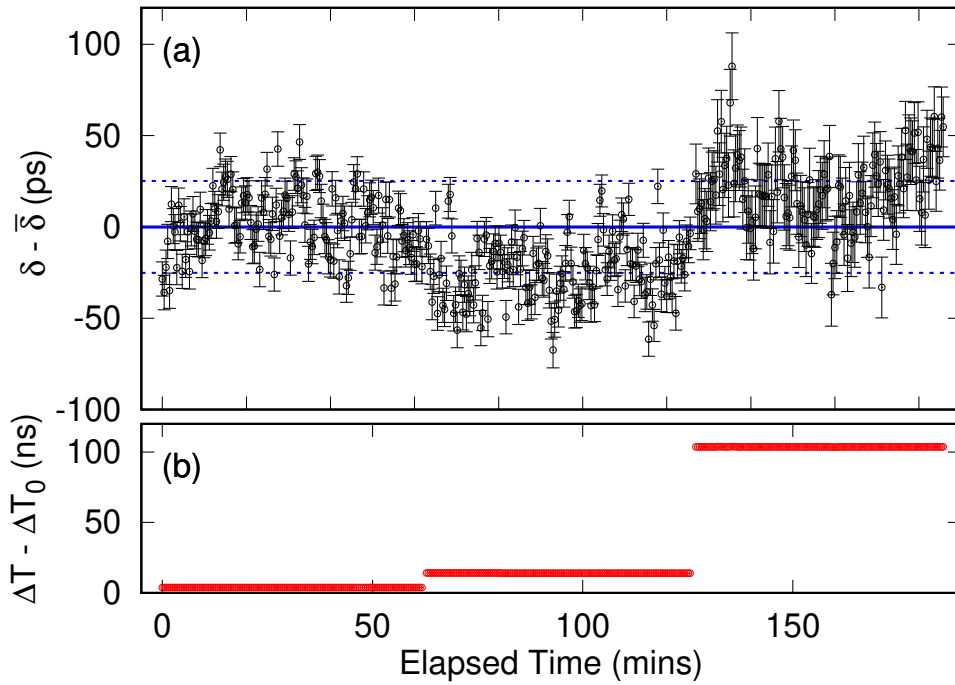
The minimum resolvable clock separation associated with the offset precision is 3.3 mm. To demonstrate that the protocol is secure against symmetric channel delay attacks, we change the propagation length over several meters during synchronization — three orders of magnitude larger than the minimum resolvable length-scale.

#### 4. Distance-independent clock synchronization with the same reference clock

To simulate a symmetric channel delay attack, we impose different propagation distances using different fiber lengths. Figure 5 shows the measured offset  $\delta$  and the round-trip time  $\Delta T$ , with an overall standard deviation of 26 ps, and an overall mean of  $\bar{\delta}$ . The sets of  $\delta$  obtained for  $L = L_0 + 1$  m and  $L_0 + 10$  m, with mean offsets  $\bar{\delta} - 24(17)$  ps, and  $\bar{\delta} + 20(20)$  ps, respectively, show significant overlap with those obtained with  $L = L_0 = 10$  km with mean offset  $\bar{\delta} + 1(17)$  ps. Comparing the additional mean offset of 19(26) ps to the additional single-trip delay (48.3 ns) expected for extending our optical channel from  $L = L_0$  to  $L_0 + 10$  m, our protocol suppresses the contribution of the additional propagation delay on the measured offset by a factor of  $\approx 4 \times 10^{-4}$ .

As the mean offset values do not appear to correlate with  $L$ , we do not attribute the differences between the mean offset values to any length-dependent mechanism. We observe however, in Fig. 5(a), that the offsets measured changed continuously and gradually even when  $L$  was changed abruptly during the the symmetric delay attack. Given these observations, and given that both timestamp units were disciplined to the same Rubidium oscillator over the entire measurement duration in Fig. 5, it is plausible that the remaining continuous offset drift can be attributed to the long-term instability of the timestamp units; the timestamp unit accuracy fluctuates due to the

256 non-uniformity of implementing timestamping bin-widths, and varies as a function of operation  
 257 time and temperature.  
 258



281 **Fig. 5.** (a) Measured offset  $\delta$  between two clocks, both locked on the same frequency  
 282 reference. The continuous line indicates the average offset  $\bar{\delta}$ . Error bars: precision  
 283 uncertainty due to errors in determining the positions,  $\tau_{AB}$  and  $\tau_{AA}$ , of the coincidence peaks.  
 284 Dashed lines: one standard deviation. (b) The round-trip time  $\Delta T$  was changed using fiber  
 285 lengths  $L = L_0 = 10$  km,  $L_0 + 1$  m, and  $L_0 + 10$  m.  $\Delta T_0 = 103.3$   $\mu$ s.

## 287 5. Distance-independent clock synchronization with independent clocks

288 To examine a more realistic scenario, we provide each time-stamping unit with an independent  
 289 frequency reference (both Stanford Research Systems FS725), resulting in a clock offset that  
 290 drifts with time  $\delta \rightarrow \delta(t)$ .

291 The frequency references each have a nominal frequency accuracy  $d_0 < 5 \times 10^{-11}$ , resulting in  
 292 a relative accuracy  $\sqrt{2} d_0$  between two clocks. We evaluate the offset from the time stamps every  
 293  $T_a = 3$  s so that the maximum expected drift ( $< 212$  ps) of the coincidence peak in  $G^{(2)}(\tau)$  is  
 294 smaller than its FWHM. This pseudo-stationary regime allows the peak positions to be extracted  
 295 with the same fitting procedure used when the clocks are locked onto the same frequency Ref.  
 296 [6].

297 We again simulate a symmetric channel delay attack using three different values of  $L$ . Figure 6  
 298 shows the measured  $\delta(t)$  which appears to follow a continuous trend over different round-trip  
 299 times, indicating that the delay attacks were ineffective. Discontinuities in  $\delta(t)$  correspond to  
 300 periods when fibers were changed.

301 To verify that meaningful clock parameters can be extracted from  $\delta(t)$  despite the attack, we  
 302 fit the data to a parabola  $a t^2 + d t + b$ , where  $a$ ,  $d$  and  $b$  represent the relative aging, frequency  
 303 accuracy and bias of the frequency references, respectively [17]. The resulting relative frequency  
 304 accuracy between the clocks,  $d = 5.1654(7) \times 10^{-11}$ , agrees with the nominal relative frequency  
 305 accuracy  $\sqrt{2} d_0$  between our frequency references. The residual of the fit,  $r(t)$  (Fig. 6(b)),

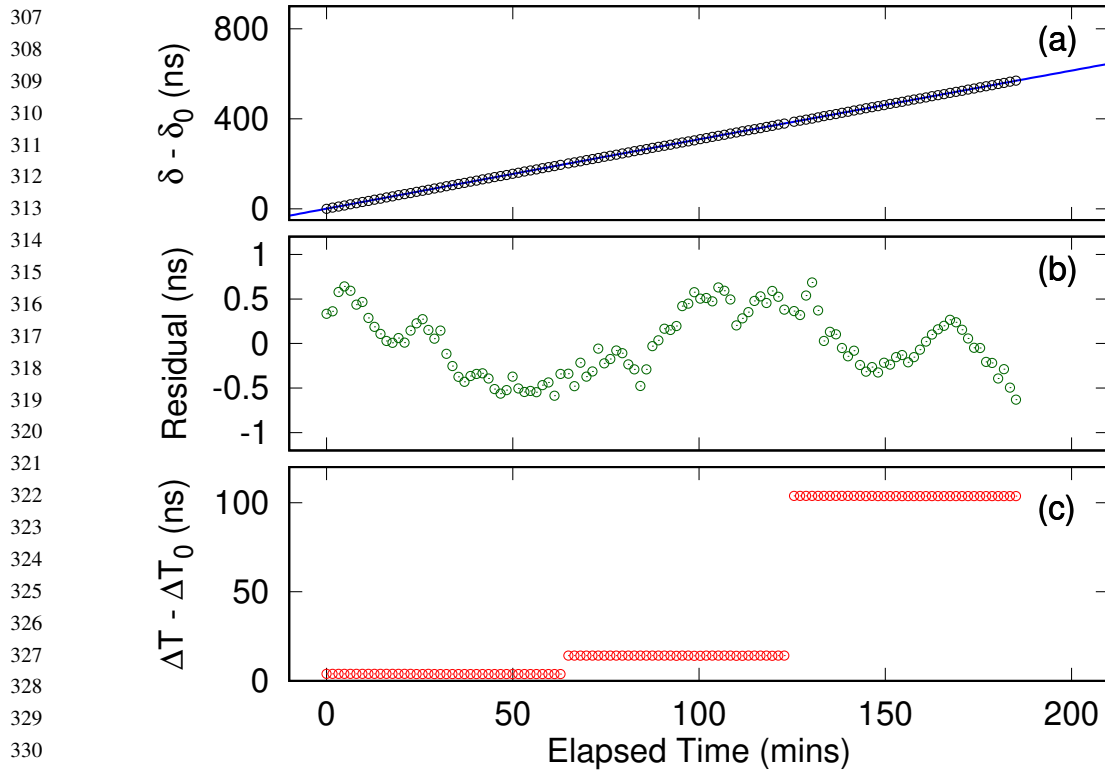


**Fig. 6.** (a) Measured offset  $\delta$  between two clocks with different frequency references. Each value of  $\delta$  was evaluated from measuring photon pair timing correlations for 3 s. The offset measured at the beginning is  $\delta_0$ . Continuous blue line: fit used to extract the relative frequency accuracy ( $\approx 5.16 \times 10^{-11}$ ) between the clocks. (b) Residual of the fit fluctuates due to the intrinsic instability of the individual frequency references. (c) The round-trip time  $\Delta T$  was changed using three different fiber lengths.

fluctuates [18] (Allan deviation =  $2.2 \times 10^{-12}$ , time deviation = 88 ps in 100 s) mainly due to the intrinsic instabilities of our frequency references ( $2 \times 10^{-12}$  in 100 s each).

The symmetric channel delay attack demonstrated in this work abruptly changed the channel length, and is similar to the attacks demonstrated in Refs. [6,7,19]. For scenarios where the channel delay is changing continuously in time, our protocol is robust against small length changes due to thermal fluctuations or mechanical vibrations. To extract the peak positions of the cross-correlation and auto-correlation distributions, we need to remain in the pseudo-stationary regime where we require that the peaks do not shift significantly compared to their widths. The upper bound to the rate  $v$  at which the channel length changes is determined by two inequalities:  $\frac{vT_a^{AB}}{u} + \sqrt{2}d_0T_a^{AB} < \text{FWHM}^{AB}$  and  $2\frac{vT_a^{AA}}{u} < \text{FWHM}^{AA}$ , where  $T_a^{AB}$ ,  $\text{FWHM}^{AB}$  and  $\frac{vT_a^{AB}}{u}$  ( $T_a^{AA}$ ,  $\text{FWHM}^{AA}$  and  $2\frac{vT_a^{AA}}{u}$ ) is the acquisition time, width and timing-shift of the cross (auto)-correlation coincidence peak,  $\sqrt{2}d_0T_a^{AB}$  the timing-shift due to the relative frequency inaccuracy between the clocks, and  $u = 2.04 \times 10^8 \text{ ms}^{-1}$  the speed of 1316 nm photons in the SMF28e fibre. Substituting the values of  $\text{FWHM}^{AB} = 905 \text{ ps}$ ,  $\text{FWHM}^{AA} = 950 \text{ ps}$ ,  $T_a^{AB} = 3 \text{ s}$  and  $T_a^{AA} = 90 \text{ s}$ , we obtain an upper bound of  $v_{max} \approx 50 \text{ mms}^{-1}$  and  $1 \text{ mms}^{-1}$  for measuring the single and round-trip times. We note that this upper bound increases with reduced acquisition times, at the expense of synchronization precision.

358

359

360

361

362

363

364

365

366

367

368

369

370

371

372

373

374

375

376

377

378

379

380

381

382

383

384

385

386

387

## 6. Protocol security

Although not demonstrated in this work, Alice and Bob can verify the origin of each photon by synchronizing with polarization-entangled photon pairs and performing a Bell measurement to check for correspondence between the local and transmitted photons. This proposal addresses the issue of spoofing in current classical synchronization protocols [6,8]. Presently, classical protocols are unable to authenticate a synchronization signal that has been delayed during an intercept, delay and resend attack when the resent signal has the same cryptographic characteristics as that of the genuine signal [5]. However, when entangled photons are used for synchronization, the same attack will, in-principle, degrade the distributed entanglement and alter the associated Bell measurement. This is a consequence of the quantum no-cloning theorem, which precludes an adversary from making an exact copy of the polarization state of the intercepted photon [20].

Due to the low coincidence-to-accidental ratio associated with the round-trip time measurement (CAR=0.13), this authentication scheme is only feasible for the single-trip time measurement (CAR=8.9). Consequently, users can only authenticate photons traveling from Alice to Bob, and have to assume that the synchronization channel has not been asymmetrically manipulated in order to incorporate the round-trip time measurement in the clock offset calculation (Eq. (3)).

In addition, we also assumed that the photon propagation times in both directions were equal ( $\Delta t_{AB} = \Delta t_{BA}$ ). Without this assumption, the offset

$$\delta = \tau_{AB} - \tau_{AA} + \Delta t_{BA} \quad (4)$$

can no longer be obtained directly from the peak positions  $\tau_{AB}$  and  $\tau_{AA}$ .

We note that an adversary will be able to exploit both assumptions while evading detection by passively rerouting photons traveling in opposite directions in the synchronization channel without disturbing their polarization states [19]. This attack is based on the fact that the momentum and polarization degree-of-freedoms of our photons are separable, and remains a security loophole in similar implementations [6,7].

## 7. Conclusion

We have demonstrated a protocol for synchronizing two spatially separated clocks absolutely with time-correlated photon pairs generated from SPDC. By assuming symmetry in the synchronization channel, the protocol does not require *a priori* knowledge of the relative distance or propagation times between two parties, providing security against symmetric channel delay attacks and timing signal authentication via the measurement of a Bell inequality [8]. Compared to previous implementations [6,7], our protocol requires only a single photon pair source, relying on the back-reflected photon to sample the round-trip time of the synchronization channel. This arrangement allows multiple parties to synchronize with bidirectional signals with a single source.

With our protocol, we synchronize two independent rubidium clocks while changing their relative separation, using telecommunication fibers of various lengths ( $\geq 10$  km) as a synchronization channel. Even with relatively modest detected coincidence rates ( $160\text{ s}^{-1}$ ) used for the round-trip time measurement, we obtained a precision sufficient to resolve clock offset fluctuations with a time deviation of 88 ps in 100 s, consistent with the intrinsic frequency instabilities of our clocks. The precision improves with detectors with lower timing jitter [7], brighter sources, or for a transmission channel with insignificant dispersion (free space). Frequency entanglement may also be leveraged to cancel dispersion non-locally, improving protocol precision over optical channels in future work [7].

**Funding.** Ministry of Education - Singapore (Research Centres of Excellence programme); National Research Foundation (Research Centres of Excellence programme).

Q1

**Acknowledgments.** We thank S-Fifteen Instruments for assistance with the entangled photon pair source and the InGaAs detector.

405

406

407

408

409

**Disclosures.** The authors declare no conflicts of interest.

410

**Data availability.** Data underlying the results presented in this paper are not publicly available at this time due to their large file size (about 310 Gb) but may be obtained from the authors upon reasonable request.

411

**References**

412

1. W. Wenjun, D. Shaowu, L. Huanxin, and Z. Hong, "Two-way satellite time and frequency transfer: Overview, recent developments and application," in *2014 European Frequency and Time Forum (EFTF)*, (IEEE, 2014), pp. 121–125.
2. D. L. Mills, "Internet time synchronization: the network time protocol," *IEEE Trans. Commun.* **39**(10), 1482–1493 (1991).
3. "Ieee standard for a precision clock synchronization protocol for networked measurement and control systems," IEC 61588:2009(E) pp. C1–274 (2009).
4. P. Moreira, J. Serrano, T. Włostowski, P. Loschmidt, and G. Gaderer, "White rabbit: Sub-nanosecond timing distribution over ethernet," in *2009 International Symposium on Precision Clock Synchronization for Measurement, Control and Communication*, (2009), pp. 1–5.
5. L. Narula and T. E. Humphreys, "Requirements for secure clock synchronization," *IEEE Journal of Selected Topics in Signal Processing* **12**(4), 749–762 (2018).
6. J. Lee, L. Shen, A. Cerè, J. Troupé, A. Lamas-Linares, and C. Kurtsiefer, "Symmetrical clock synchronization with time-correlated photon pairs," *Appl. Phys. Lett.* **114**(10), 101102 (2019).
7. F. Hou, R. Quan, R. Dong, X. Xiang, B. Li, T. Liu, X. Yang, H. Li, L. You, Z. Wang, and S. Zhang, "Fiber-optic two-way quantum time transfer with frequency-entangled pulses," *Phys. Rev. A* **100**(2), 023849 (2019).
8. A. Lamas-Linares and J. Troupé, "Secure quantum clock synchronization," *Proc. SPIE* **10547**, 105470L (2018).
9. R. Quan, H. Hong, W. Xue, H. Quan, W. Zhao, X. Xiang, Y. Liu, M. Cao, T. Liu, S. Zhang, and R. Dong, "Implementation of field two-way quantum synchronization of distant clocks across a 7 km deployed fiber link," *Opt. Express* **30**(7), 10269–10279 (2022).
10. C.-K. Hong, Z.-Y. Ou, and L. Mandel, "Measurement of subpicosecond time intervals between two photons by interference," *Phys. Rev. Lett.* **59**(18), 2044–2046 (1987).
11. R. J. Glauber, "The quantum theory of optical coherence," *Phys. Rev.* **130**(6), 2529–2539 (1963).
12. Y. Shi, S. Moe Thar, H. S. Poh, J. A. Grieve, C. Kurtsiefer, and A. Ling, "Stable polarization entanglement based quantum key distribution over a deployed metropolitan fiber," *Appl. Phys. Lett.* **117**(12), 124002 (2020).
13. A. Lohrmann, C. Perumangatt, A. Villar, and A. Ling, "Broadband pumped polarization entangled photon-pair source in a linear beam displacement interferometer," *Appl. Phys. Lett.* **116**(2), 021101 (2020).
14. J. A. Grieve, Y. Shi, H. S. Poh, C. Kurtsiefer, and A. Ling, "Characterizing nonlocal dispersion compensation in deployed telecommunications fiber," *Appl. Phys. Lett.* **114**(13), 131106 (2019).
15. C. Ho, A. Lamas-Linares, and C. Kurtsiefer, "Clock synchronization by remote detection of correlated photon pairs," *New J. Phys.* **11**(4), 045011 (2009).
16. M. Bousonville and J. Rausch, "Velocity of signal delay changes in fibre optic cables," in *Proceedings of the Ninth European Workshop on Beam Diagnostics and Instrumentation for Particle Accelerators (DIPAC)*, (2009).
17. G. Xu and Y. Xu, *GPS, Theory, Algorithms and Applications* (Springer Berlin Heidelberg, Berlin, Heidelberg, 2016).
18. W. J. Riley, *Handbook of frequency stability analysis* (US Department of Commerce, National Institute of Standards and Technology, 2008).
19. J. Lee, L. Shen, A. Cerè, J. Troupé, A. Lamas-Linares, and C. Kurtsiefer, "Asymmetric delay attack on an entanglement-based bidirectional clock synchronization protocol," *Appl. Phys. Lett.* **115**(14), 141101 (2019).
20. W. K. Wootters and W. H. Zurek, "A single quantum cannot be cloned," *Nature* **299**(5886), 802–803 (1982).

444

445

446

447

448

449

450

451

452

453

454

455

456

457

458

459